Long-term perspective on wildfires in the western USA

Jennifer R. Marlon[a,1], Patrick J. Bartlein[b], Daniel G. Gavin[b], Colin J. Long[c], R. Scott Anderson[d], Christy E. Briles[e], Kendrick J. Brown[f], Daniele Colombaroli[g], Douglas J. Hallett[h], Mitchell J. Power[i], Elizabeth A. Scharf[j], and Megan K. Walsh[k]

[a]Department of Geography, University of Wisconsin, Madison, WI 53706; [b]Department of Geography, University of Oregon, Eugene, OR 97403; [c]Department of Geography and Urban Planning, University of Wisconsin, Oshkosh, WI 54901; [d]School of Earth Sciences and Environmental Sustainability, Northern Arizona University, Flagstaff, AZ 86011; [e]School of Geography and Environmental Science, Monash University, Victoria 3800, Australia; [f]Canadian Forest Service, Victoria, BC, Canada V8Z 1M5; [g]Oeschger Centre for Climate Change Research and Institute of Plant Sciences, University of Bern, Altenbergrain 21, CH-3013 Bern, Switzerland; [h]Biogeoscience Institute, University of Calgary, Alberta, Canada T2N 1N4; [i]Natural History Museum of Utah, Department of Geography, University of Utah, Salt Lake City, UT 84112; [j]Department of Anthropology, University of North Dakota, Grand Forks, ND 58202; and [k]Department of Geography, Central Washington University, Ellensburg, WA 98926

Edited by B. L. Turner, Arizona State University, Tempe, AZ, and approved January 10, 2012 (received for review August 13, 2011)

Understanding the causes and consequences of wildfires in forests of the western United States requires integrated information about fire, climate changes, and human activity on multiple temporal scales. We use sedimentary charcoal accumulation rates to construct long-term variations in fire during the past 3,000 y in the American West and compare this record to independent fire-history data from historical records and fire scars. There has been a slight decline in burning over the past 3,000 y, with the lowest levels attained during the 20th century and during the Little Ice Age (LIA, ca. 1400–1700 CE [Common Era]). Prominent peaks in forest fires occurred during the Medieval Climate Anomaly (ca. 950–1250 CE) and during the 1800s. Analysis of climate reconstructions beginning from 500 CE and population data show that temperature and drought predict changes in biomass burning up to the late 1800s CE. Since the late 1800s , human activities and the ecological effects of recent high fire activity caused a large, abrupt decline in burning similar to the LIA fire decline. Consequently, there is now a forest "fire deficit" in the western United States attributable to the combined effects of human activities, ecological, and climate changes. Large fires in the late 20th and 21st century fires have begun to address the fire deficit, but it is continuing to grow.

Forest fires in the western United States have been increasing in size (1) and possibly severity (2) for several decades. The increase in fire has prompted multiple investigations into both the causes (3, 4) and consequences of this shift for communities, ecosystems, and climate (5). Climate changes and human activities have both contributed to the observed changes in fire, but understanding the nature and magnitude of these impacts has been challenging first because there is substantial ecological heterogeneity and variability in terms of vegetation, soils, hydrology, topography, and other factors that affect fire regimes across the western United States, and second because most fire-history data come from recent decades and centuries when climate and human activities have both undergone rapid and unique transformations. As a result, studies tend to focus either on local ecological and anthropogenic factors that drive fire at fine scales (6, 7), or on climatic influences at broad scales (3, 4). Furthermore, the limited temporal scope of many fire-history studies does not provide adequate context for examining the joint impacts of climate and human activities on broad-scale, long-term fire regime changes. In addition, projections of future climate change and its ecosystem impacts place the expected changes well outside the range of variations in the past few centuries. Thus, coupling multi-decadal-to millennial-scale data on fire, climate changes, and human activities can reveal linkages among these components that are often missed in studies restricted to finer scales or fewer factors.

Here we use sedimentary charcoal accumulation rates to construct variations in levels of burning for the past 3,000 y in the western United States (i.e., the West) and compare this record to independent fire-history data from historical records and fire scars. The long charcoal records enable identification of baseline shifts in fire regimes that cannot be detected with shorter records and allow us to view the nature and extent of human impacts on fire in a long-term context; this approach helps to distill the dominant patterns in fire activity across the West, but it does not reveal the important differences in fire controls and effects among vegetation types, ecoregions, or elevation gradients that exist at finer spatial scales (e.g., ref. 8).

Our focus here is specifically on multi-decadal-to-centennial-scale variations in fire over the past few millennia and on the West as a whole. Climatic variations on this time scale are characterized by extended periods of persistent anomalies, such as the Medieval Climate Anomaly (MCA) and Little Ice Age (LIA) (9, 10), which feature broad-scale (i.e., across the whole of the western United States) anomalies of both surface climates and atmospheric circulation (10). We use temperature (10), drought (9), and population (11) data to compare with the fire-history reconstructions. We also construct a simple statistical model for predicting biomass burning from the temperature and drought data. Our analysis builds on the rich historical narratives of fire in the western United States (12) as well as on many more detailed but shorter broad-scale studies (4, 13, 14). The results illustrate the importance of climate in explaining the variations in fire over time, and show the development of a 20th century "fire deficit" related to the combined effects of fire exclusion, land-use change, and ongoing climate change.

Broad-Scale Controls on Fire

Fire regimes are primarily a product of climate, vegetation, topography, and human activities—factors that interact in a variety of ways and on a range of spatial and temporal scales. Climate influences fire at the broadest scales via the annual cycle, weather, and the distribution of vegetation (fuels). Humans have a broad influence on fire through intentional or accidental ignitions, exclusion (e.g., suppression and fuel alteration from grazing), and indirectly through climate change. Topography, winds, and the type, distribution, and structure of vegetation become more important controls on fire at regional-to-local scales. Feedbacks from fire to vegetation and climate add additional complexity to ecosystem dynamics. Increases in human-caused fires, for ex-

Author contributions: J.R.M. and P.J.B. designed research; J.R.M., P.J.B., D.G.G., C.J.L., R.S.A., C.E.B., K.J.B., D.C., D.J.H., M.J.P., E.A.S., and M.K.W. performed research; J.R.M. and P.J.B. analyzed data; and J.R.M., P.J.B., D.G.G., C.J.L., R.S.A., C.E.B., K.J.B., D.C., D.J.H., M.J.P., E.A.S., and M.K.W. wrote the paper.

The authors declare no conflict of interest.

This article is a PNAS Direct Submission.

Freely available online through the PNAS open access option.

Data deposition: The charcoal records were collected from the Global Charcoal Database/International Multiproxy Paleofire Database.

[1]To whom correspondence should be addressed. E-mail: jennmarlon@gmail.com.

See Author Summary on page 3203 (volume 109, number 9).

This article contains supporting information online at www.pnas.org/lookup/suppl/doi:10.1073/pnas.1112839109/-/DCSupplemental.

ample, can trigger changes in the structure and composition of vegetation, which may in turn alter carbon storage and land surface characteristics that are known to affect climate (15). Furthermore, interactions among fire and its primary controls —particularly climate and vegetation—often involve lag times that span years, decades, and even centuries (16), making long-term data on fire-regime changes a vital component of fire research.

Despite major human influences on western U.S. wildfires since Euro-American settlement (17, 18), climate is generally considered to be the primary control on fire in the region (1, 3, 4, 14, 19). The processes by which concurrent climate and vegetation conditions support or suppress fire vary by scale. On seasonal-to-interannual time scales, field observations and satellite data have demonstrated the importance of temperature, the variability of precipitation, and drought in controlling patterns of burning (1, 3, 20). Given sufficient vegetation productivity (21), high temperatures and drought are consistently linked with greater area burned and with large fire years in the West (22, 23). Fire activity in dry shrublands and grasslands is also strongly linked with antecedent precipitation that drives the development of fine fuels necessary for the spread of large fires in these ecosystems (24, 25). High temperatures during the fire season promote fire-conducive weather and lightning ignitions, but temperature is also important in the spring and fall because it extends the fire season (1, 4). In winter, high temperatures reduce snowpack, which affects soil (and fuel) moisture (1). The effects of temperature on fire apply on centennial (4) and longer time scales (26) as well. In any given year, the spatial distributions of areas burned are highly irregular, although organized temporally by weather variations (27).

Field observations and longer dendrochronological fire-scar records demonstrate the importance of El Niño Southern Oscillation (ENSO) on interannual climate variability (28), particularly in the southwestern United States (22). ENSO creates a dipole pattern in the western United States characterized by opposing climate conditions in the northwest and the southwest. During La Niña events, ocean surface temperatures are cold in the eastern equatorial Pacific and the southwest tends to receive reduced precipitation and have abundant fires (29); the northwest tends to be wetter-than-normal and to have few fires (30). During El Niño events climate and fire conditions are reversed from La Niña conditions (22). La Niña conditions were a contributing factor to the large fires in Texas and Arizona this year (2011) in June, for example. Despite the prominence of this dipole pattern in discussions in the fire science literature, the most important mode of interannual variability of climate is a region-wide pattern of anomalies of similar (rather than opposing) sign for temperature and precipitation (31), snowpack (32), and the timing of snowmelt runoff (33), as reflected by the first principal component of each dataset.

On decadal-to-centennial scales, fire patterns have been linked to slow changes in ocean/atmosphere patterns associated with low-frequency variations in sea surface temperatures (14, 23). Most work has focused specifically on linking fire patterns to ocean/atmosphere dynamics associated with the Pacific Decadal Oscillation (34) and/or the Atlantic Multidecadal Oscillation (14). Fire patterns during the 20th century for example show that large fire years are associated with a strong, persistent trough over the northeastern Pacific Ocean and an associated ridge over the West Coast, which leads to subsidence and thus dry conditions in all western U.S. forests (23). Years with few fires are associated with a weakened Aleutian Low, high sea surface temperatures in the central North Pacific, a stronger-than-normal jet stream, and low geopotential heights that combine to produce wet conditions in the West (4).

Our knowledge of millennial-scale changes in fire activity comes primarily from sedimentary charcoal data, which shows the strong influence of annual temperature and summer drought (35, 36). Vegetation productivity (37) and changes in forest composition and structure [e.g., related to succession (38, 39)] are also an important control on fire regimes in many parts of the United States at centennial and millennial time scales. The magnitude of variation in climate and fire analyzed here are beyond the range of the instrumental and historical records of the 20th and 21st centuries, but they are still smaller in amplitude than those projected to occur over the next century.

Human impacts on forest fires in the western United States since Euro-American settlement are well documented and primarily resulted from altered ignition patterns associated with land and debris clearance, agriculture, fire suppression, and fire exclusion more broadly. Grazing and the introduction of nonnative species had major impacts on a host of ecological processes that affect fire, including forest composition and structure, nutrient cycling, soils, and hydrology. Many studies document such human impacts on fire at local scales (40–42), but the scale of earlier impacts from indigenous burning are still debated [e.g., (43)]. Temporal variability in indigenous fire impacts likely occurred across two spatial scales: locally within individual populations (i.e., within territories of indigenous cultural groups), and across larger areas related to longer-term cultural changes. There is good evidence for local effects on vegetation and fire history from fossil charcoal, pollen, and archaeological data (44–46), but little evidence for widespread impacts, which we focus on here and index by regional population levels for lack of more nuanced synthetic or continuous data.

Our analyses provide convergent evidence from charcoal, historical, and tree-ring data for trends in fire activity during recent centuries; they also show that the variations in charcoal over the interval between 500 and 1800 CE (Common Era) are explained by variations in temperature and drought. We then use the charcoal data to characterize fire history for the past three millennia across the western United States The spatial scale of our study matches that of climatic and human impacts on fire today, and the long-term perspective allows us to study the response of fire regimes to a wide range of climate and human influences.

Sources of Fire-History Data and Their Treatment

Each type of fire-history data has unique strengths and weaknesses in terms of spatial and temporal coverage. Detailed estimates of recent fires, area and/or biomass burned are available from remote sensing and historical records (24, 47), but these data span a few decades at most. Longer historical reconstructions inferred from documents, photographs, ethnographic records, or other archives tend to focus on the most destructive fires and rarely provide evidence of broad changes in fire regimes; an exception to this is the unique historical record created by the United States Department of Agriculture (USDA) Forest Service in order to estimate the extent, use, and destruction of original saw timber stand (i.e., trees older than 50 y in 1630 CE) across the United States through the period of historic settlement (48, 49). The data include regional estimates of the original stand, amount cut, destruction and regrowth, and remainder. The data are provided by decade from 1630–1940 CE (Fig. 1, 48). We scale these estimates of widespread disturbance by the percent destruction in the western regions to obtain estimates of western U.S. fires over time. While the report's estimates are inevitably coarse, the level of detail available for selected years and areas suggests that substantial effort and care went into compiling the data. These early data can be supplemented and indirectly validated by examining stand-establishment data derived from forest inventories from the western United States (50). Such data document the course of establishment and reforestation following the widespread disturbances associated with historic settlement.

Cross-dated fire-scar records provide a consistent long-term history of fire frequency over centuries, and in rare cases millennia (51–54). Fire-scar data however are only available in forests that do not typically experience stand-replacing fires (52). Stand-

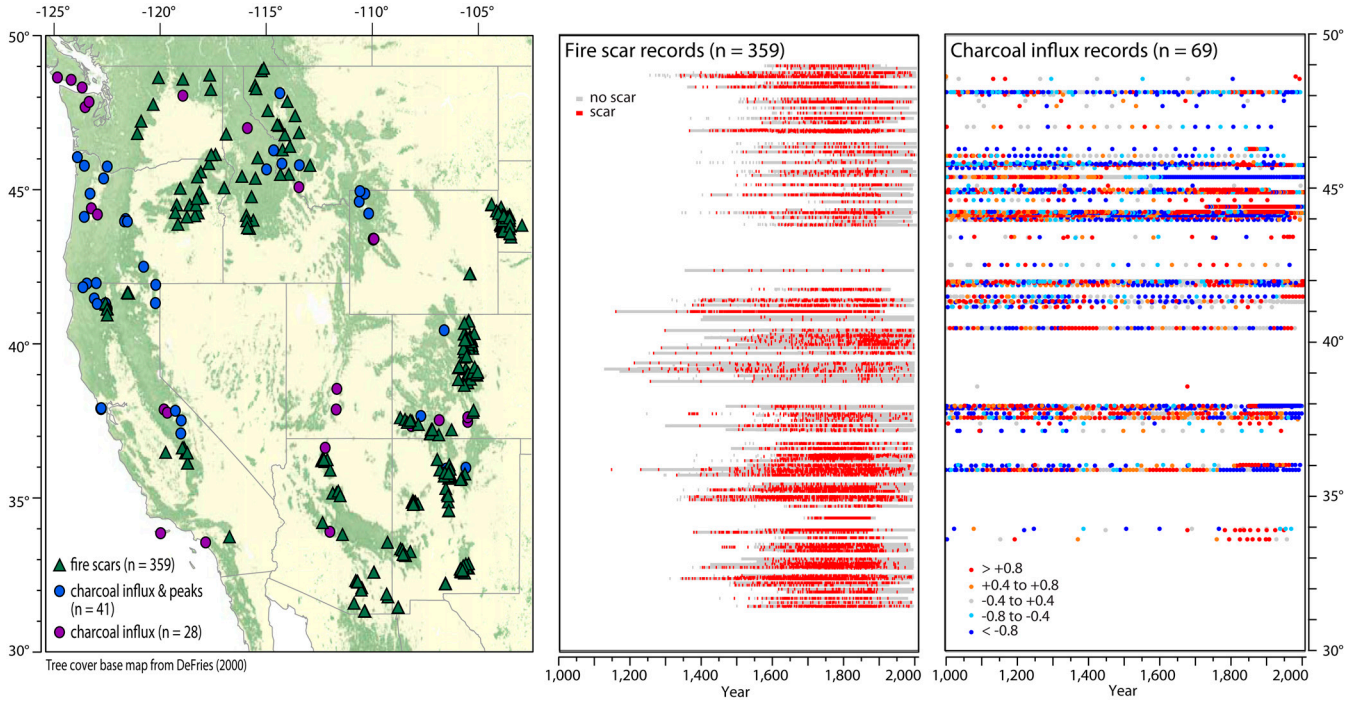


Fig. 1. (*A*) The geographic distribution of fire-scar (green triangles) records and charcoal-based fire-history records (influx and peak frequency records are blue, influx-only records are purple) in the western United States on a base map of tree cover (84); (*B*) The latitudinal distribution of dendrochronological sites recording fire scars for the past 1,000 y. A site is gray when it is recording fire, and a red tick mark indicates a fire scar (URL: http://www.ncdc.noaa.gov/paleo/impd/paleofire.html); isolated gray tick marks at the beginning of each record indicate the beginnings of individual tree records. (*C*) Anomalies of charcoal influx over the past 1,000 y from 69 sites in the western United States arranged latitudinally from north (top) to south (bottom). Each row represents a study site. Blue dots indicate less burning than average; red dots indicate more burning than average. Spacing of the dots reflects the sampling resolution and sedimentation rate of the record.

age data can be used to reconstruct fire history in such forests [e.g., (55)], but stand-age data are temporally more limited because only the most recent fire can be dated at each site. The International Multiproxy Paleofire Database (IMPD*) contains annually-resolved fire scars from over 350 sites (Fig. 1). The number of sites recording fires varies from year to year in this dataset, so we calculated the proportion of recording sites with ≥1 and ≥2 scars for each year (Fig. 2*B*). Changes in the proportion of sites with fire scars in a given year were summarized (see *Methods*, *SI Text*) to illustrate widespread trends in fire incidence (56) regardless of size or synchrony throughout the western United States.

Charcoal data are the most widespread proxy for fire occurrence and biomass burned on decadal-to-millennial time scales. Composites of multiple charcoal accumulation rate (influx) records have been shown to reflect coherent regional trends in biomass and area burned (37, 39). We obtained 48 charcoal records from the Global Charcoal Database version 1 (57) plus 21 recently published records (Table S1). The 69 charcoal records (Fig. 1) were converted to influx data and standardized using a protocol designed to facilitate intersite comparisons and synthesis (58) (Fig. 2*C*). A subset of 41 high-resolution records were further analyzed by decomposing the charcoal data into "background" and "peak" or "fire-episode" time series (59). Peak time series were then composited into a region-wide summary of peak densities, reflecting broad-scale changes in fire frequencies (Fig. 2*D*).

The differences in historical, fire scar, and charcoal datasets make direct comparisons challenging (see *SI Text*), particularly at the local scale, where past analyses have produced mixed results [e.g., (35, 39, 54, 60)]. At broad scales, however, the differences in fire-scar and charcoal data are an asset, allowing more spatially and temporally comprehensive reconstructions of fire history than is possible with either type of data alone.

Results and Discussion

Historical Evidence of Fire in the West. The western United States is comprised of four regions in the USDA historical dataset: the North and South Pacific and the North and South Rocky Mountains. The original (*ca.* 1700 CE) stand volume for these four regions together was estimated to be 2.24×10^9 board feet (bf, 1,000 bf = 2.36 m^3), with about 73% in the north and 27% in the south. The "original" forest in the western United States accounted for about 18% (58.7 million hectares) of the total original U.S. forest area, whereas the remaining stand in 1940 accounted for about 66% of the total forested area in the United States.

Historical records of national timber resources document the increasing impacts on forests from Euro-American fuelwood use, lumbering, and land clearing across the country (Fig. S1). Fire use also increased (Fig. 2*A*). Information on regional differences in timber use and damage are not available, but the primary spatial pattern of Euro-American impacts on fire likely followed the westward expansion of the frontier from the Missouri River *ca.* 1830 to its final close by the early 1900s. The recovery or reforestation following the widespread disturbance of the 1800s can be seen in stand-age data from forest inventories from the western United States (Fig. S1). These data show a modal year of stand origin in the first decade of the 20th century, with half the stands originating between 1870 and 1950 CE.

Fire-Scar and Charcoal-Based Evidence of Fire in the West. All the fire-scar data and most of the charcoal data come from forested ecosystems (Fig. 1*A*; Fig. S2). Fire-scar records ($n = 369$ sites, >50,000 individual scars) are more evenly distributed between north and south than the charcoal data, but there are more

*http://www.ncdc.noaa.gov/paleo/impd/.

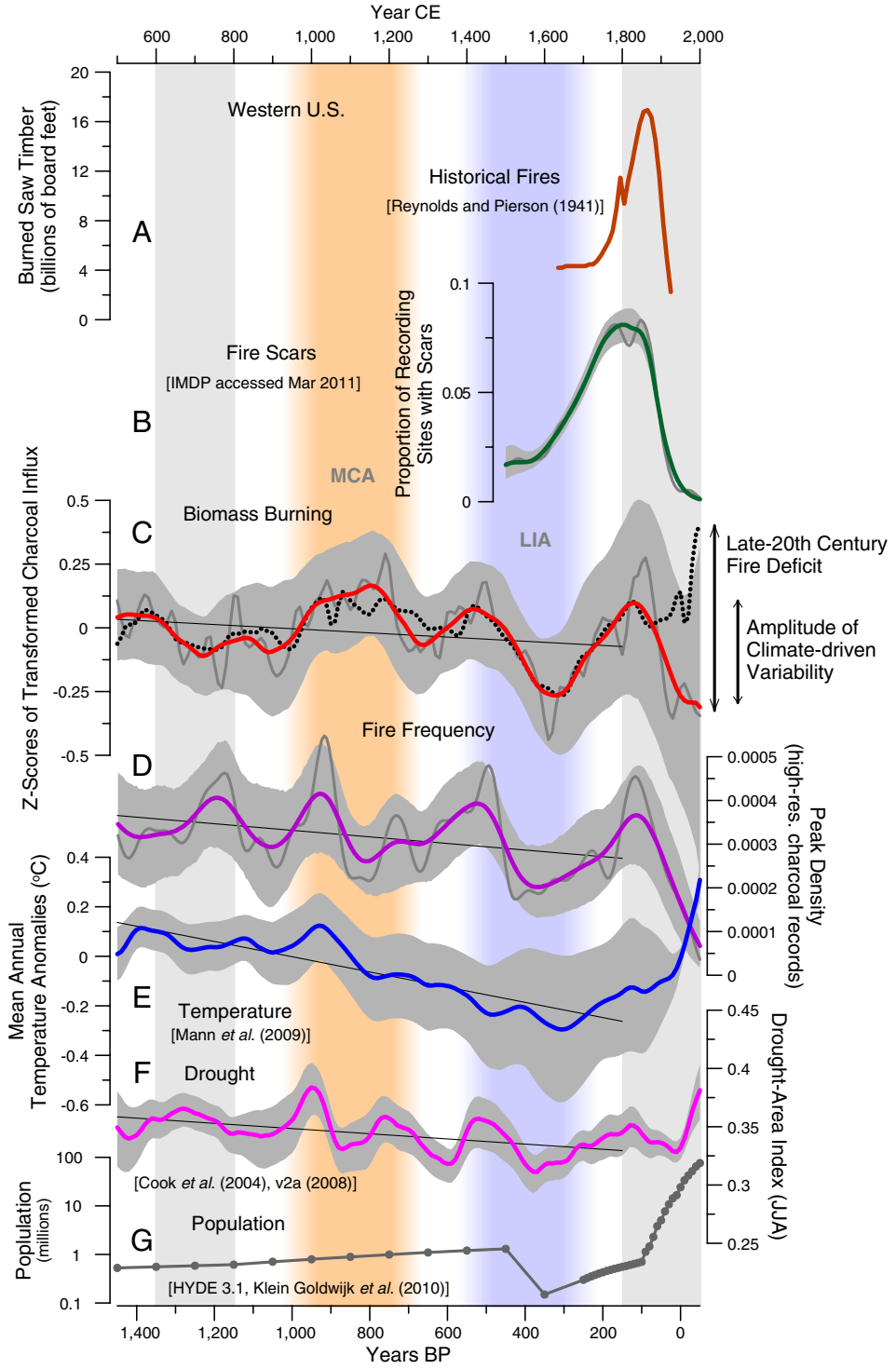


Fig. 2. (*A*) Estimated historical saw timber affected by fires (48). (*B*) Smoothed proportions of dendrochronological sites recording fire scars (the green curve is based on locally fitting nearest-neighbor parameter of 0.25, while the gray curve is based on a parameter value of 0.10. (*C*) Smoothed and standardized 25-year (gray) and 100-year (red) trend line through standardized biomass burning records ($n = 69$) along with predicted biomass burning based on a GAM (black dashed line) fit to the 100-year biomass burning records. (*D*) Smoothed peak density (inferred fire frequency) from charcoal values ($n = 41$). (*E*) Smoothed gridded temperature anomalies for the western United States (10). (*F*) Smoothed Palmer Drought Severity Index for the western United States (9) . (*G*) Population estimates for the western United States (11). All smoothed curves are plotted with 95% bootstrap confidence intervals.

fire-scar data from low-and midelevation xeric interior forests of the Rocky Mountains than in the higher elevations or more mesic forests, although some data do come from less xeric/midelevation forests; e.g., in Colorado (61) (Fig. 1*A*). In addition, fires do not always leave scars, especially in forests with high fire frequencies and on young trees, so the fire-scar data likely underestimates true fire frequency (62). General patterns in the fire-scar data however, should be robust. For example, it is clear that northern sites tend to burn less frequently than southern sites (Fig. 1*C*, Fig. S2), and fires were more frequent from *ca.* 1600 to 1900 CE than after that interval. Specific years when widespread fires occurred are evident when the fire-scar records are not overlap-

ping (Fig. S2). Widespread fires are easier to identify in the northwest in part because there are fewer fires in general, but there also appears to be greater fire synchrony in the north than in the south in general. Widespread fires occur fairly regularly during the high fire period from 1600–1900 CE, but an increase in small fires is also evident from *ca.* 1850 through the early 1900s (most visible in central and northern records; Fig. S2). The most salient feature of the fire-scar data is the widespread, abrupt reduction in fires around 1900 CE.

Charcoal data from the West are more prevalent in the north (where lakes are more common) than in the south (Fig. 1*C*). Charcoal influx rates (CHAR) vary continuously during the past 1,000 y at most sites, although the nature of within-record variability differs from site to site. Some records show low CHAR for the past millennium followed by high CHAR during historic settlement, for example, whereas other records show high variability from decade to decade. In many records there is a tendency toward high CHAR between 1100–1200 CE, between 1800–1900 CE, and in the most recent samples. Low CHAR are common *ca.* 500 y ago, particularly in the north.

A temporal summary of the fire-scar data (Fig. 2*B*; Figs. S3 and S4) shows that the proportion of sites recording scars increased from about 1400–1800 CE, with a broad maximum between 1800 and 1850. The earliest part of this trend (i.e., prior to *ca.* 1500 CE) is more uncertain than latter parts, however, because (*i*) fewer sites were recording fire activity early in the millennium, so the data reflect changes in burning at fewer than 40 locations, and (*ii*) the early increase in the proportion of sites recording scars may partly reflect an increasing number of trees susceptible to fire scarring at each site (63). Comparison of analyses using either one or more or two or more scars to indicate fire years across the West as a whole, as well as for the north and south show that trends in fire activity summarized with this method are robust to alternative minimum scarring criteria (Fig. S4).

Combining the 69 charcoal influx records (Fig. 2*C*; Fig. 3) provides an indication of the trends and variability in biomass burning across the western United States during the past 3,000 y. Burning declined slightly over the past 3,000 y, with the lowest levels attained during the LIA, (*ca.* 1400–1700 CE/550-250 cal y BP) and in the 20th century. Peaks in burning occurred during the MCA (*ca.* 950–1250 CE/1000-700 cal y BP) and during the 1800s CE (Fig. 3). There is a large and rapid shift from high burning in the 19th century to low burning in the 20th century that is comparable in magnitude to the decline in fire that occurred during the transition into the LIA.

Charcoal peak density shows distinct maxima similar to the composite charcoal influx record over the past 1,500 y (Fig. 2 *C* and *D*). The sharpest maxima in peak frequency occur at the beginning of the MCA and LIA, and, as was the case for the other records, during the early 1800s; smaller maxima occur at the ends of the MCA and LIA. The association of peak density maxima with rapid or large warming or cooling events is consistent with that observed during deglaciation (64), and during the last glacial interval (65); increased fire at these times would be supported by vegetation changes that increase fuels available for combustion (e.g., due to increased mortality).

Climatic and Human Influences on Fire in the West. Mean annual temperature (MAT) and summer drought (drought-area index, DAI) were summarized in a similar fashion to the charcoal data (see *Methods*) and also show a general downward trend, at least until the early 1800s (Fig. 2 *A–D*). The long-term decline in fire is also evident for the 1,500 y prior to the beginning of the joint record at 500 CE (Fig. 3). Superimposed on this trend are several large and generally parallel variations in biomass burning and fire frequency (i.e., "fire activity") during the past 2,000 y (Fig. 2 *C* and *D*). Fire activity was high at 1000, 1400, and 1800 CE, and low at 900, 1600, and 1900 CE. The rise in fire at 1000 CE occurred at the beginning of the MCA, when temperatures (MAT) and drought area (DAI) were both high. Biomass burning remained high for at least two centuries during the MCA (from 750 to 1000 cal y CE), whereas fire frequency declined at 1100 CE. Another increase in fire activity occurred at the beginning of the LIA around 1400 CE, when drought increased rapidly. Biomass burning reached its late Holocene minimum during the LIA, and fire-episode frequency was also low at this time, although it is presently lower. The decline in fire activity during the LIA occurred as drought declined and temperatures reached their 1,500-y minimum (Fig. 2 *E* and *F*). Similar trends and centennial-scale variability in climate and fire until the 1800s suggests that baseline levels of fire activity in the West were predominantly controlled by climate.

High fire activity during the MCA has been documented by individual local studies based on both fire-scar and charcoal records [e.g., (54, 66)], and our results indicate that such activity was widespread. Biomass burning was high throughout the MCA and peaked at 1200 CE during a period of severe drought; the level of

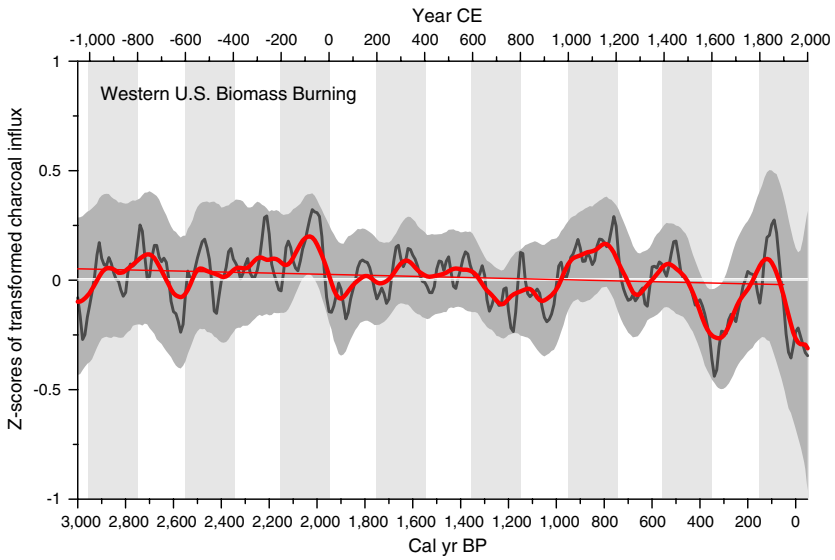


Fig. 3. Relative changes in biomass burning in the western United States for the past 3,000 y based on 69 standardized sedimentary charcoal records. The red line is a lowess curve based on a 200-year window width and the dark gray line is a lowess curve based on a 100-year window. 95% bootstrap confidence intervals are shown as a gray band.

burning then was similar to that reached about a century ago (during historic settlement). Fire frequency also reached a peak during the MCA at *ca.* 1000 CE, when both drought and temperatures were particularly high. Fire frequency in the West was higher at this time than at any other time in the past 1,000 y. Warm, dry conditions in the western United States during the MCA resulted from prevailing La Niña-like conditions in the tropical Pacific, which is consistent with both increased drought and high temperatures (Fig. 2 *E* and *F*) (10, 67).

Biomass burning and fire frequency were also high during the transition into the LIA, during a prolonged period of severe drought (Fig. 2*E*); fire then declines to minimum levels at 1500 CE and *ca.* 1575 CE for fire frequency and biomass burning, respectively (Fig. 2 *C* and *D*). The fire-scar record becomes dense enough to analyze during the LIA and indicates very low levels of fire activity then. Evidence from glacial advances in the Sierra Nevada range of California and the Cascade Range of the Pacific Northwest (68) suggest decreases in summer temperature during the LIA of ~2 °C in Sierra Nevada (69). Native American populations also collapse after approximately 1,500 CE, which would have significantly reduced the impact from human-caused fires where they were important previously (Fig. 2*G*). The combination of low values for drought, temperature, population, biomass burning, and fire frequency during the LIA suggest that multiple factors, including reduced vegetation productivity from lower temperatures, reduced fire-conducive weather (wetter conditions), and fewer human-caused fires to some extent, combined to reduce fire activity generally during the LIA.

The charcoal influx record over the past 3,000 y (Fig. 3) indicates that variations in biomass burning have been particularly large over the past 1,000 y. The negative excursions in biomass burning during the LIA and in the past century for example, are remarkable in the context of the past 3,000 y. In general however, large shifts in the magnitude and rate of burning have occurred throughout the past. For example, there is an abrupt decrease of charcoal influx around 2,000 y ago comparable to the first step in the decrease between the MCA and LIA, and there is a gradual increase commencing around 1300 CE that is analogous to that leading into the MCA. There are several features of the charcoal records that are not well explained by climate, for example the maximum in peak density around 800 CE, but overall, until the 1800s, increases in temperature and drought are coeval with increases in charcoal influx and peak density.

To further quantify the relationship between biomass burning and climate, we developed a statistical regression model (Generalized Additive Model or GAM; Fig. S3). The regression was fit using centennial changes in biomass burning from temperature and DAI from 500 to 1800 AD (i.e., from the beginning of the joint temperature and drought records to settlement). Climate explains most of the multidecadal to century-scale variations of biomass burning ($R^2 = 0.85$; $F = 47.0$; $p < 0.001$). Temperature alone can account for half of the total variance of biomass burning ($R^2 = 0.53$; $F = 51.2$; $p < 0.001$), while drought area can explain about one-third of the overall variance ($R^2 = 0.34$; $F = 24.4$; $p < 0.001$). The dashed black curve on Fig. 2*C* shows the fitted (to 1800 CE) and predicted (1800–2000 CE) values from the model (see also Fig. S5). The general features of the influx record are captured, including the upturn in influx at the end of the LIA, and a subsequent peak in biomass burning around 1800 CE. The observed and predicted influx curves diverge after 1800 CE, when the combined effects of landscape fragmentation and fire exclusion reduced biomass burning in the face of post-LIA and 20th century temperature increases. Because the model was fit only to data prior to 1800 CE, we checked whether the predictions over the past 200 y are extrapolations beyond the range of the calibration data (Fig. S6). The values of the predictor (climate) variables fall outside the general envelope of climate values only after 1980 CE, so the divergence between observed and predicted charcoal influx beginning in the 1800s CE is most likely due to nonclimatic controls.

Prior to the 1800s and within the temporal and spatial scales of this study, human activity, expressed as population from the HYDE 3.1 database (Fig. 2*G*), does not appear to influence either the charcoal influx or peak density variations. Population gradually increased (in contrast to biomass burning, which decreased) until after 1500 CE, when European contact resulted in an abrupt population decline owing to disruptions such as disease and warfare (70). Although the low levels of biomass burning attained throughout the Americas during the LIA are often ascribed to contact (71, 72), the general decline in biomass burning was underway before contact [e.g., (26)], and seems largely accounted for by climate. The divergence between the observed and predicted (by climate) charcoal influx curves after 1800 CE is thus the main expression of human impacts on fire.

During the transition out of the LIA and into the Settlement Era, historical records, fire-scar, and charcoal data (both observed and predicted) track increasing temperatures and drought, showing a multicentury increase in forest fire activity from very low levels during the LIA to very high levels of burning between 1700 and 1900 CE (Fig. 2 *A–D*).

The close association between observed and predicted biomass burning prior to the late 1800 s suggests that climate changes alone can explain the increase in fire activity between 1600 and 1800 CE. The more variable (25-year smoothed) biomass burning curve (Fig. 2*C*, thin gray line) however, shows that fire activity increased to very high levels in the 1800s despite an apparently earlier decline in observed and predicted biomass burning (Fig. 2*C*). The peak in fire activity in the mid to late 1800s is undoubtedly due in part to increased human-caused burning, which reaches its maximum from 1850–1870 CE (Fig. 2*A*). Settlers arriving in the western United States at this time ignited many fires for clearing forest and brush, lumbering, railroad construction, agriculture, arson, etc. Road building and technological advances were also linked to increased anthropogenic burning (and erosion), such as with the development of steam power and railroads that created sparks leading to large numbers of wildfires until the early 1900s (when the railroads were required to start clearing woodlands within 100 feet of tracks to prevent fires). The introduction of the band saw in 1880 CE, and powerful logging machinery in 1890 CE, for example, also led to changes in harvesting that further altered forests and fuels as well as the locations of intentional and accidental fires. Increased anthropogenic burning in the west from 1850–1900 CE is widely recognized in dendrochronological studies (61), but increased variability in moisture availability associated with ENSO also contributed to increased burning then (74).

Prior to the arrival of large numbers of Euro-Americans in the western United States, the fire-history records show a short-lived decline in fire in the 1810s CE. The annual fire-scar data indicate that this decline in burning was driven by very low fire activity in the years 1816 and 1818 CE; only 13 sites record scars in 1816 and 15 sites in 1818 compared with a century-long average of 36 sites. These results are consistent with the hypothesized effects of widespread cooling following the eruption of Mount Tambora in 1815 CE (75).

Observed and predicted changes in biomass burning begin to diverge in the late 1800s creating a fire deficit that has been growing throughout the 20th century (Fig. 2*C*). Predicted biomass burning generally rises from the late 1800s CE to present, consistent with increased temperature and drought trends. In contrast, observed biomass burning, as well as fire scars, charcoal-based fire frequencies, and human-caused fires decline rapidly. The minimum in burning during the 20th century is similar to the low fire activity levels that occurred during the LIA. Less than 10% of the original sawtimber stand remained at that point, mostly on the Pacific Coast (48), so while it is plausible that a reduction in forest

cover contributed to reduced burning, this seems unlikely because timber extraction and destruction does not necessarily lessen wildfire risk, and in some cases increases it (76).

Multiple factors combined to cause the 20th century fire decline (77), largely due to human activities but also due to ecological processes following the intensive fire activity in the 1800s. Grazing was perhaps the earliest primary cause of fire exclusion in the West. Hundreds of thousands of livestock were introduced to pine forests and grasslands in western states (40, 42) in the late 1800s. The widespread herds reduced grassy fuel loads, compacted soils, and sharply reduced fire frequencies. Road and trail building also created fire breaks that limited the natural spread of fires. Cultural changes were also taking place that may have reduced fire ignitions well before effective fire suppression in the 1940s. By 1900 CE, the western frontier had largely closed and several large catastrophic fires, such as the Peshtigo Fire in Wisconsin in 1871 that killed over one thousand people (78) were helping to change attitudes towards fire and fire policies. In 1891, the Forest Reserve Act was introduced that allowed the President to reserve forests from the public domain (79), and in 1905 the U.S. Forest Service was established with a primary mission of suppressing all fires that occurred on reserved lands. Responsibility for fire management was transferred from the Army to the National Park Service when it was created in 1916, and full suppression remained the policy for the next five decades (with greatly increased efficiency in the 1940s) (79). Natural ecosystem changes also likely contributed to decreased fire in the 1900s, however. Increased fire in the late 19th century, for example, resulted in young stands in subalpine forest that were less susceptible to fire in the early 20th century. A major increase in fire-resistant aspen stands due to 19th century fires also likely reduced biomass burning and fire frequencies.

In general, western U.S. forests were fundamentally changed in the 1800 and 1900s from previous centuries. The increased burning of the 1800s and the subsequent widespread exclusion of fire altered stand structure and composition, understory vegetation and fuel loads, and facilitated entry of nonnative species (76). Coupled with timber extraction and land clearance, the consequences for western forests were dramatic.

The fire deficit identified here might appear to contrast with observations of recent increases in western U.S. fire activity (1) and also to the well established fire-climate interactions documented across the region (14). These apparent differences can be reconciled by explicit consideration of the time scale of the variations. We show that mean or baseline levels of biomass burned and fire frequency decreased substantially during the past century compared with previous centuries; the recent increase in "fire activity" (i.e., large-wildfire occurrence) is therefore occurring during a period of unusually low levels of biomass burning. Furthermore, the increase observed since 1980 has a short duration compared with the longer decline in burning from the 19th to 20th centuries, or increases at the beginning of the MCA or following the LIA. Similarly, the associations between large fire occurrence, fire frequency, and climate that are well documented in literature on western U.S. fire regimes (61, 80) are also dependent on scale and fire-regime dimension; interannual and even multidecadal fire synchrony for example, may have been as strong in the past as they are today with no "decoupling" of fire and climate on these time scales. During the past two centuries, however, centennial-scale changes in biomass burned and fire frequency however, *are* decoupled from climate due to the strong human influences on forests and fires.

Although the changes in fire described here were undoubtedly widespread, our results do not address several important aspects of fire history of the western United States. First, the trends do not reflect subregional patterns of burning or changes in burning in grasslands and shrublands. A good example is the increase in area burned in California during the 20th century. Area burned has expanded consistently during the past 100 y as a result of increasing population growth and drought (81, 82), however this pattern is not reflected in the composite curve due to a lack of paleofire data from that state. Second, differences in interannual to decadal-scale variations in burning such as those due to ENSO are also not reflected in our data. Third, the recent increases in large wildfires across western states also do not appear in the composite tree-ring or charcoal summaries, most likely because their occurrence is too recent to be incorporated into most sediments or fire-scar records. However, increases in fire are evident in individual charcoal records, particularly from the northern forests (Fig. 1).

Conclusions

Biomass burning in the western United States has remained in dynamic equilibrium with climate at least since 500 CE to the 1800s CE. Burning generally increased when temperatures and drought area increased, and decreased when temperatures and drought declined. The onset of persistent century-scale climate anomalies like the MCA and LIA are marked by peaks in fire-episode frequency and gradually increasing biomass burning levels during warm intervals and generally decreasing levels during cool intervals; this is consistent with observations on longer time scales that abrupt climate changes, toward either warmer or cooler conditions are marked by peaks in biomass burning (although peaks are larger when the shift is toward warmer conditions).

Against the backdrop of climatic and ecological processes, human activities had a marked impact on biomass burning after the late 1800s. Our synthesis distills the dominant patterns in human impacts, but it does not reveal the large spatial differences in fire controls and effects, such as those that vary with vegetation type and elevation gradients, that are necessary to inform management and restoration efforts (8), which, if applied uncritically, can result in collateral damage (83). The data do suggest however that even modest increases in temperature and drought (relative to those being projected for the 21st century) are able to perturb the level of biomass burning as much as large-scale industrialized human impacts on fire.

More dramatic increases in temperature or drought are likely to produce a response in fire regimes that are beyond those observed during the past 3,000 y. Since the mid 1800s, the trend in fire activity has strongly diverged from the trend predicted by climate alone and current levels of fire activity are clearly out of equilibrium with contemporary climate conditions. The divergence in fire and climate since the mid 1800s CE has created a fire deficit in the West that is jointly attributable to human activities and climate change and unsustainable given the current trajectory of climate change.

Based on the fire data alone, the levels of burning during the 19th and 20th centuries are not anomalous; there were times (i.e., the LIA) when fire was as low as it has been over much of the 20th century, and times when it was as high as during the 1800s, as around 50 to 1 BCE. When climate is considered however, the past approximately 150 y (i.e., back to 1850) are remarkably anomalous. Although the current rate of biomass burning is not unusual (even allowing for post-1980 CE increases in burning such as in ref. 3), it is clearly out of equilibrium with the current climate. Our long-term perspective shows that the magnitude of the 20th century fire decline, while large, was matched by "natural" fire reduction during cold, moist intervals in the past (e.g., LIA). Current fire exclusion and suppression however, is taking place under conditions that are warmer and drier than those that occurred during the MCA, which calls into question their long-term efficacy.

Finally, the historical, dendrochronological and charcoal records are in accordance when examined from similar temporal and spatial perspectives. The different records each provide unique information on particular scales of variation and their causal mechanisms. Given the size of the current fire deficit and its

potential to grow in the future, the unique perspectives provided by each data source will be necessary for projecting the response of fire in the western United States to both ongoing and future climate changes.

Methods

We used historical, fire-scar, and charcoal data to construct three independent records of millennial-and centennial-scale trends in fire occurrence across the entire west. Historical data were obtained from Reynolds and Pierson (48), and from Littell, et al. (3). All fire-scar data available in the IMPD[†] were used but only injuries to the trees defined by the data contributor as a fire scar were used in the analysis. We calculated the proportion of recording sites with scars each year, and summarized them using a locally fitted binomial logit model with bootstrap confidence intervals.

Charcoal data were obtained from the Global Charcoal Database [GCD version 1 (57)] and authors (Table S1). Age estimates for data in the GCD were taken as-is and were not modified or improved. For charcoal analyses, concentration data (particles cm^{-3}) were converted to influx values (particles cm^{-2} y^{-1}) and were then standardized using methods described in detail in Power, et al. (58). The transformed and standardized influx data were summarized (Fig. 2*C*) using locally weighted regression (lowess). Bootstrap confidence intervals were calculated by resampling (with replacement, 1,000 replications) the charcoal data by site (as opposed to by sample) in order to illustrate the uncertainty of the smoothed values to the particular distribution of sites in the dataset.

A subset of high-resolution records were analyzed using CharAnalysis (59), which separates peaks from background charcoal (*SI Text*). The binary peak (or fire-event series were summarized using a kernel density estimator (Fig. 2*D*), and again bootstrap confidence intervals were calculated by resampling by site (*SI Text*).

Temperature data were obtained from Mann, et al. (10) (Fig. 2*E*). The temperature time series, expressed as anomalies from a 1960–1990 CE long-term mean, was smoothed using the same approach taken with the charcoal data (i.e., lowess smoothing based on a 100-y window width), and bootstrap confidence intervals were calculated in a similar fashion, by resampling the individual grid-cell time series. The drought reconstruction (Fig. 2*F*) uses data from Cook, et al. (9) to calculate a region-wide DAI [i.e., the proportion of grid cells with PDSI (Palmer Drought-Severity Index) values less than −1.0]. The DAI data were also smoothed using the same approach as the charcoal data, with a 100-y smoothing window width. Population estimates for the western United States were derived from the HYDE 3.1 dataset (11) (Fig. 2*G*). Population time series were generated by aerially averaging gridded HYDE data for the western US.

ACKNOWLEDGMENTS. We thank Jeremy Littell and two anonymous reviewers for manuscript comments. We greatly appreciate the contributors to the International Multiproxy Paleofire Database and the Global Charcoal Database. We also thank Brad Smith from the USDA Forest Service for the historical fire data. Support for this study was provided by a National Science Foundation Grants ATM-0714146 to P.J.B., SBR-9700544 to E.A.S., and Postdoctoral Fellowship EAR-0948288 to J.R.M.

[†]http://www.ncdc.noaa.gov/paleo/impd/.

1. Westerling AL, Hidalgo HG, Cayan DR, Swetnam TW (2006) Warming and earlier spring increase western US forest wildfire activity. *Science* 313:940–943.
2. Miller J, Safford H, Crimmins M, Thode A (2009) Quantitative evidence for increasing forest fire severity in the Sierra Nevada and Southern Cascade Mountains, California and Nevada, USA. *Ecosystems* 12:16–32.
3. Littell JS, McKenzie D, Peterson DL, Westerling AL (2009) Climate and wildfire area burned in western U. S. ecoprovinces, 1916-2003. *Ecol Appl* 19:1003–1021, doi: 10.1890/07-1183.1.
4. Trouet V, Taylor AH, Wahl ER, Skinner CN, Stephens SL (2010) Fire-climate interactions in the American West since 1400 CE. *Geophys Res Lett* 37:L04702.
5. Wiedinmyer C, Neff J (2007) Estimates of CO_2 from fires in the United States: implications for carbon management. *Carbon Balance and Management* 2, doi: 10.1186/1750-0680-1182-1110.
6. Odion DC, et al. (2004) Patterns of fire severity and forest conditions in the western Klamath Mountains, California. *Conserv Biol* 18:927–936.
7. Taylor AH (2007) *Forest changes since Euro-American Settlement and ecosystem restoration in the Lake Taho Basin* (PSW-GTR-203, USDA Forest Service, USA).
8. Baker WL, Veblen TT, Sherriff RL (2007) Fire, fuels and restoration of ponderosa pine-Douglas fir forests in the Rocky Mountains, USA. *J Biogeogr* 34:251–269.
9. Cook ER, Woodhouse CA, Eakin CM, Meko DM, Stahle DW (2004) Long-term aridity changes in the western United States. *Science* 306:1015–1018.
10. Mann ME, et al. (2009) Global signatures and dynamical origins of the Little Ice Age and Medieval Climate Anomaly. *Science* 326:1256–1260.
11. Klein Goldewijk K, Beusen A, Janssen P (2010) Long-term dynamic modeling of global population and built-up area in a spatially explicit way: HYDE 3.1. *Holocene* 20:565–573.
12. Pyne SJ (1997) *America's Fires: Management of Wildlands and Forests* (Forest History Society, Durham, NC).
13. Swetnam TW, Baisan CH (1996) Historical fire regime patterns in the southwestern United States since AD 1700. *Second La Mesa Fire Symposium, March 29-31, 1994*, ed CD Allen (Department of Agriculture, US), pp 11–32.
14. Kitzberger T, Brown PM, Heyerdahl EK, Swetnam TW, Veblen TT (2007) Contingent Pacific-Atlantic ocean influence on multi-century wildfire synchrony over western North America. *Proc Nat'l Acad Sci USA* 104:543–548.
15. Hurteau MD, Brooks ML (2011) Short-and long-term effects of fire on carbon US dry temperate forest systems. *BioScience* 61:139–146.
16. Whitlock C, Higuera PE, McWethy DB, Briles CE (2010) Paleoecological perspective on fire ecology: revisiting the fire regime concept. *The Open Ecology Journal* 3:6–23.
17. Covington WW, Moore MM (1994) Southwestern ponderosa forest structure and resource conditions: changes since Euro-American settlement. *J Forest* 92:39–47.
18. Taylor AH, Skinner CN (2003) Spatial patterns and controls on historical fire regimes and forest structure in the Klamath Mountains. *Ecol Appl* 13:704–719.
19. Whitlock C, Shafer SL, Marlon J (2003) The role of climate and vegetation change in shaping past and future fire regimes in the northwestern US and the implications for ecosystem management. *Forest Ecol Manag* 178:5–21.
20. van der Werf GR, et al. (2010) Global fire emissions and the contribution of deforestation, savanna, forest, agricultural, and peat fires (1997–2009). *Atmos Chem Phys* 10:11707–11735.
21. Krawchuk MA, Moritz MA (2011) Constraints on global fire activity vary across a resource gradient. *Ecology* 92:121–132.
22. Swetnam TW, Betancourt JL (1990) Fire-southern oscillation relations in the southwestern United States. *Science* 249:1017–1021.
23. Trouet V, Taylor AH, Carleton AM, Skinner CN (2006) Fire-climate interactions in forests of the American Pacific coast. *Geophys Res Lett* 33:L18704.
24. Westerling AL, Gershunov A, Brown TJ, Cayan DR, Dettinger MD (2003) Climate and wildfire in the western United States. *B Am Meteorol Soc* 84:595–604.
25. Brown KJ, et al. (2005) Fire cycles in North American interior grasslands and their relation to prairie drought. *Proc Nat'l Acad Sci USA* 102:8865–8871.
26. Marlon J, et al. (2008) Climate and human influences on global biomass burning over the past two millennia. *Nature Geosci* 1:697–701.
27. Bartlein P, Hostetler SW, Shafer SL, Holman JO, Solomon AM (2008) Temporal and spatial structure in a daily wildfire-start dataset from the western United States (1986–96). *Int J Wildland Fire* 17:8–17.
28. Gedalof Z, Peterson DL, Mantua NJ (2005) Atmospheric, climatic, and ecological controls on extreme wildfire years in the northwestern United States. *Ecol Appl* 15:154–174.
29. Swetnam TW, Baisan CH (2003) Tree-ring reconstructions of fire and climate history in the Sierra Nevada and southwestern United States. *Fire and climate in temperate ecosystems of the western Americas*, eds TT Veblen, WL Baker, G Montenegro, and TW Swetnam (Springer-Verlag, New York), pp 158–195.
30. Heyerdahl EK, Morgan P, Riser JP, II (2008) Multi-season climate synchronized widespread historical fires in dry forests (1650–1900), Northern Rockies, USA. *Ecology* 89:705–716.
31. Diaz HF, Fulbright DC (1981) Eigenvector analysis of seasonal temperature, precipitation and synoptic-scale system frequency over the continguous United States Part I: Winter. *Mon Weather Rev* 109:1267–1284.
32. McCabe GJ, Dettinger MD (2002) Primary modes and predictability of year-to-year snowpack variations in the western United States from teleconnections with Pacific Ocean climate. *J Hydrometeorol* 3:13–25.
33. Stewart IT, Cayan DR, Dettinger MD (2005) Changes toward earlier streamflow timing across western North America. *J Climate* 18:1136–1155.
34. Hessl A, McKenzie D, Schellhaas R (2004) Drought and Pacific decadal oscillation linked to fire occurrence in the inland Pacific Northwest. *Ecol Appl* 14:425–442.
35. Brunelle A, Whitlock C, Bartlein P, Kipfmueller K (2005) Holocene fire and vegetation along environmental gradients in the Northern Rocky Mountains. *Quaternary Sci Rev* 24:2281–2300.
36. Minckley T, Whitlock C, Bartlein P (2007) Vegetation, fire, and climate history of the northwestern Great Basin during the last 14,000 years. *Quaternary Sci Rev* 26:2167–2184.
37. Marlon J, Bartlein PJ, Whitlock C (2006) Fire-fuel-climate linkages in the northwestern USA during the Holocene. *Holocene* 16:1059–1071.
38. Kipfmueller K, Kupfer JA (2005) Complexity of successional pathways in subalpine forests of the Selway-Bitterroot Wilderness Area. *Ann Assoc Am Geogr* 95:495–510.
39. Higuera PE, Whitlock C, Gage JA (2010) Linking tree-ring and sediment-charcoal records to reconstruct fire occurrence and area burned in subalpine forests of Yellowstone National Park, USA. *Holocene* 21:327–341.
40. Savage M, Swetnam TW (1990) Early 19th-century fire decline following sheep pasturing in a Navajo ponderosa pine forest. *Ecology* 71:2374–2378.
41. Anderson R, Carpenter S (1991) Vegetation change in Yosemite Valley, Yosemite National Park, California during the protohistoric period. *Madroño* 38:1–13, http://www.bioone.org/toc/madr/58/2.
42. Heyerdahl EK, Brubaker LB, Agee JK (2001) Factors controlling spatial variation in historical fire regimes: a multiscale example from the interior West, USA. *Ecology* 82:660–678.

43. Vale T (2002) *Fire, Native Peoples, and the Natural Landscape* (Island Press, Washington) p 315.
44. Roos C, Sullivan A, III, McNamee C, eds. (2010) *Paleoecological Evidence for Indigenous Burning in the Upland Southwest* (Southern Illinois University, Carbondale), pp 142–171.
45. Scharf EA (2010) A statistical evaluation of the relative influences of climate, vegetation, and prehistoric human population on the charcoal record of Five Lakes, Washington (USA). *Quatern Int* 215:74–86.
46. Walsh MK, Whitlock C, Bartlein PJ (2010) 1200 years of fire and vegetation history in the Willamette Valley, Oregon and Washington, reconstructed using high-resolution macroscopic charcoal and pollen analysis. *Palaeogeogr Palaeocl* 297:273–289.
47. Giglio L, Randerson JT, van der Werf GR, Collatz GJ, Kasibhatla P (2006) Global estimation of burned area using MODIS active fire observations. *Atmos Chem Phys Discussions* 5:11091–11141.
48. Reynolds RV, Pierson AH (1941) The saw timber resource of the United States,1630–1930. *Forest Survey Release 53* (USDA Forest Service, Washington, DC).
49. Birdsey RA, Pregitzer K, Lucier A (2006) Forest carbon management in the United States: 1600–2100. *J Environ Qual* 35:1461–1469.
50. Hicke JA, Jenkins JC, Ojima DS, Ducey M (2007) Spatial patterns of forest characteristics in the western United States derived from inventories. *Ecol Appl* 17:2387–2402.
51. Swetnam TW (1993) Fire history and climate change in giant sequoia groves. *Science* 262:885–889.
52. Kipfmueller K, Baker WL (2000) A fire history of a subalpine forest in south-eastern Wyoming, USA. *J Biogeogr* 27:71–85.
53. Kitzberger T, Swetnam TW, Veblen TT (2001) Inter-hemispheric synchrony of forest fires and the El Niño-Southern Oscillation. *Global Ecol Biogeogr* 10:315–326.
54. Swetnam TW, et al. (2009) Multi-millennial fire history of the giant forest, Sequoia National Park, USA. *Fire Ecology* 5:120–148.
55. Johnson EA, Gutsell SL (1994) Fire frequency models, methods and interpretations. *Adv Ecol Res* 25:239–283.
56. Veblen TT, Kitzberger T, Villalba R, Donnegan J (1999) Fire history in northern Patagonia: The roles of humans and climatic variation. *Ecol Monogr* 69:47–67.
57. Power MJ, et al. (2008) Changes in fire regimes since the Last Glacial Maximum: an assessment based on a global synthesis and analysis of charcoal data. *Clim Dynam* 30:887–907.
58. Power MJ, Marlon JR, Bartlein PJ, Harrison SP (2010) Fire history and the Global Charcoal Database: a new tool for hypothesis testing and data exploration. *Palaeogeogr Palaeocl* 291:52–59.
59. Higuera P, Gavin D, Bartlein P, Hallett D (2010) Peak detection in sediment-charcoal records: impacts of alternative data analysis methods on fire-history interpretations. *Int J Wildland Fire* 19:996–1014.
60. Allen CD, Anderson RS, Jass RB, Toney JL, Baisan CH (2008) Paired charcoal and tree-ring records of high-frequency Holocene fire from two New Mexico bog sites. *Int J Wildland Fire* 17:115–130.
61. Veblen TT, Kitzberger T, Donnegan J (2000) Climatic and human influences on fire regimes in ponderosa pine forests in the Colorado Front Range. *Ecol Appl* 10:1178–1195.
62. Baker W, Ehle D (2001) Uncertainty in surface-fire history: the case of ponderosa pine forests in the western United States. *Canadian Journal for Forest Resources* 31:1205–1226.
63. Van Horne ML, Fulé PZ (2006) Comparing methods of reconstructing fire history using fire scars in a southwestern United States ponderosa pine forest. *Canadian Journal for Forest Resources* 36:855–867.
64. Marlon J, et al. (2009) Wildfire responses to abrupt climate change in North America. *Proc Nat'l Acad Sci USA* 106:2519–2524.
65. Daniau A-L, et al. (2007) Dansgaard-Oeschger climatic variability revealed by fire emissions in southwestern Iberia. *Quaternary Sci Rev* 26:1369–1383.
66. Colombaroli D, Gavin D (2010) Highly episodic fire and erosion regime over the past 2,000 y in the Siskiyou Mountains, Oregon. *Proc Nat'l Acad Sci USA* 107:18909–18914.
67. Trouet V, et al. (2009) Persistent positive North Atlantic Oscillation mode dominated the Medieval Climate Anomaly. *Science* 324, doi:10.1126/science.1166349):78-80.
68. Osborn G, Luckman BH (1988) Holocene glacier fluctuations in the Canadian Cordillera (Alberta and British Columbia). *Quaternary Sci Rev* 7:115–128.
69. Bowerman ND, Clark DH (2011) Holocene glaciation of the central Sierra Nevada, California. *Quaternary Sci Rev* 30:1067–1085.
70. Denevan WM (1992) *The Native Population of the Americas in 1492* (University of Wisconsin Press, Madison, WI) p 404.
71. Dull RA, et al. (2010) The Columbian encounter and the Little Ice Age: Abrupt land use change, fire, and greenhouse forcing. *Ann Assoc Am Geogr* 100:755–771.
72. Nevle RJ, Bird DK (2008) Effects of syn-pandemic fire reduction and reforestation in the tropical Americas on atmospheric CO_2 during European conquest. *Palaeogeogr Palaeocl* 264:25–38.
74. Veblen TT, Kitzberger T (2002) Inter-hemispheric comparison of fire history: The Colorado Front Range, USA., and the Northern Patagonian Andes, Argentina. *Plant Ecol* 163:187–207.
75. Swetnam TW, Brown PM (2011) Climatic inferences from dendoecological reconstructions. *Dendroclimatology Progress and Prospects*, eds MK Hughes, TW Swetnam, and HF Diaz (Springer, Dordrecht), pp 263–295.
76. Keeley JE, et al. (2009) *Ecological Foundations for Fire Management in North American Forest and Shrubland Ecosystems* (USDA Forest Service, Pacific Northwest Research Station PNW-GTR-779, Seattle, WA).
77. Wallenius T (2011) Major decline in fires in coniferous forests—reconstructing the phenomenon and seeking for the cause. *Silva Fenn* 45:139–155.
78. Gess D, Lutz W (2002) *Firestorm at Peshtigo: A town, its people, and the deadliest fire in American history* (Holt, New York).
79. Pyne SJ (1995) *World Fire: The Culture of Fire on Earth (* (University of Washington Press, Seattle, WA) p 384.
80. Schoennagel T, Veblen TT, Kulakowski D, Holz A (2007) Multidecadal climate variability and interactions among Pacific and Atlantic sea surface temperature anomalies affect subalpine fire occurrence, western Colorado (USA). *Ecology* 88:2891–2902.
81. Keeley JE (2004) Impact of antecedent climate on fire regimes in coastal California. *Int J Wildland Fire* 13:173–182.
82. Stephens SL, Martin RE, Clinton NE (2007) Prehistoric fire area and emissions from California's forests, woodlands, shrublands, and grasslands. *Forest Ecol Manag* 251:205–216.
83. Schoennagel T, Veblen TT, Romme WH (2004) The interaction of fire, fuels, and climate across Rocky Mountain forests. *BioScience* 54:661–676.
84. DeFries R, Hansen M, Townshend JRG, Janetos AC, Loveland TR (2000) A new global 1km dataset of percent tree cover derived from remote sensing. *Global Change Biol* 6:247–254.

Supporting Information

Marlon et al. 10.1073/pnas.1112839109

SI Text

Data Analysis Methods. ***Historical records.*** Historical data are from Reynolds and Pierson (Fig. S1, 1). The whole-U.S. estimates suggest that about 60% of the original sawtimber stand at 1700 was destroyed by either natural or human causes and 40% was used. Of the 40% used, about half was for fuelwood. The trends in use and destruction, which are for the United States as a whole, indicate that farm clearing accelerated earliest, but occurred primarily in the East (2). Extraction of wood for lumber and fuelwood was more important in the West, and both accelerated rapidly in the 1800s. Fuelwood use peaked around 1875 CE, where lumber extraction continued to rise rapidly until the early 1900s, after which it declined rapidly.

Estimates of billions of board feet (bf) destroyed by fire were provided for the United States as a whole. In order to obtain an estimate of fire destruction solely for the western United States, we scaled the national data by a factor of 0.14 based on the proportion of the original stand estimates assigned to the western subregions, which were comprised of the North and South Pacific and Northern and Southern Rocky Mountains. A simple rescaling of the burned timber based on the proportion of bf in western vs. eastern regions does not take important factors such as area burned into account (e.g., in terms of stand acreage, 18% was assigned to the west vs. 82% to the east), however our focus here on temporal trends in burning should not be strongly affected by scaling factors (Fig. S1).

We also digitized stand-origin age data from Hicke et al. (3) to validate the Reynolds and Pierson historical data. These data were derived from forest-inventory databases for the western United States and include information on the age of the inventoried forest stands. These stand-origin ages illustrate the pulse of regeneration accompanying the forest loss reported by Reynolds and Pierson (Fig. S1, green curve).

Compositing, smoothing and bootstrapping the tree-ring fire-scar, charcoal influx and charcoal-peak/fire-episode data. Because our objective is to focus on region-wide, multi-decadal-to-century time scale variations in fire, we adopted a data-analytical approach that involved the construction of smooth composite curves based on the individual datasets described below. The construction of composite curves allows the common underlying variation among individual records to emerge in the composite. If there were no underlying common variation, then the variation in the individual records would "wash out" in the composite, leaving no clear long-term trend. Conversely, if there is some common pattern of temporal variation in the data, the individual records will reinforce one another, and that pattern will emerge in the composite. Because we are focusing on decadal and longer time-scale variations, temporally smoothing the data is also appropriate. In the approach we implement here, we adopted the locally weighted regression approach, as described by Cleveland (32) and Loader (7), using an appropriate model-fitting procedure for each dataset. This approach simultaneously composites the data from individual records and smooths them.

Because the data points are irregularly distributed around the region, an obvious question can be asked about the potential for individual records or groups of records to disproportionately dominate the composite. To examine the impact of individual records (in the case of the fire-scar, charcoal-influx, and charcoal-peak/fire-episode data), or individual grid points (in the case of the temperature and DAI data) we adopted a bootstrapping-by-site (as opposed to bootstrapping-by-samples) with replacement approach. The width of the bootstrap 0.05 and 0.95 confidence intervals constructed using 1,000 replications of sampling with replacement, provides a visual assessment of the impact of individual records on the composite curve. Marlon et al. (31) discuss further the general smoothing and bootstrapping approaches used here, and compare the local regression approach with alternatives such as smoothing splines.

To permit comparisons among the resulting composite curves, we obtained fitted values at even 10-year "target points." The selection of this particular interval is not intended as a statement of our belief in the underlying temporal resolution of the individual records, but instead as a practical step in the comparison of the individual composite curves.

Tree-ring fire-scar data. Fire-scar data are from the International Multiproxy Paleofire Database (URL: http://www.ncdc.noaa.gov/paleo/impd/paleofire.html). The dataset includes 1.37 million recording tree rings, which contain 52,667 individual scars, of which 50,456 (96%) were identified in particular as fire scars. These data are shown plotted in latitudinal order in Fig. S2, where each row represents a site, with a tick mark plotted each year, in red if any trees were noted as having been scarred in a particular year, and in gray otherwise. Because the number of sites recording fire activity varies over time, the proportion of sites recording fire during each year (Fig. S3) was calculated to serve as a proxy of changes in fire frequency through time for the entire region. The plots show that the fire-scar data becomes sparser going back in time, particularly prior to 1500 CE. The scatter plot of proportion of recording sites with scars by year shows distinct patterns prior to this time, related to the small number of sites in the dataset.

Because the probability of a tree recording a fire greatly increases after its initial fire-scar event (becoming a "recorder tree"), an increase in time alone may lead to an increasing number of recording trees, and that in turn increases the likelihood that any given fire will be recorded (4). Analysis of sampling methods and fire-scar accumulation curves by dendrochronologists, however, shows that there is a threshold of trees (e.g., $n = 50$) beyond which results are robust with respect to additional sampling (5). Fires in the IMDP dataset were identified by individual scars at each site, but in the absence of additional detailed analyses of the sampling methods at each site, we rely on evidence that the accumulation of fire scars from spatial networks of tree-ring records provides a reasonable proxy for region-wide fire history [e.g., (6)].

The proportion of sites recording fires was summarized using a local regression (logit) model [locfit, (7)]. We used the binomial local likelihood family (appropriate for data that are proportions), the tricube weight function, and nearest-neighbor fractions of 0.1 and 0.25. To determine the range of years over which the local regression provides an adequate summary of the data, we performed the standard diagnostic analyses of residuals, which confirmed that 1500 CE was an appropriate cutoff for plotting and examining the summary.

In order to ensure that our summary of the tree-ring data is robust, we compared local regression models of the IMPD dataset using both one or more and two or more scars as criteria. We did this for the region as a whole (Fig. S4, top box) and for the north (Fig. S4 middle box) and the south (Fig. S4 bottom box). Using two or more scars slightly reduces the overall proportion of sites recording a fire, but all three summaries yield similar patterns and demonstrate that the trends (including a dip in fire activity *ca*. 1815) are robust. We also compared analyses based on

all injuries vs. only those injuries identified as fire scars, and the results were nearly indistinguishable.

Examination of individual fire-scar and charcoal records reveals the spatial and temporal heterogeneity in the data as well as the key differences between the two types of records (Fig. 1). For example, the fire-scar records highlight increased fire frequencies at southern vs. northern sites (Fig. 1*C*), whereas regular sampling of the continuously varying charcoal accumulations highlights the dynamic nature of fire on centennial to millennial scales (Fig. 2*C*). The fire-scar data indicate how synchrony in fire regimes can occur across wide areas in specific years (Fig. S2), but even then not all sites will burn. Similarly, charcoal records indicate that peaks and troughs in biomass burning at the regional scale (Fig. 2*D*) are not supported by similar trends at all sites (Fig. 1*B*), but rather indicate intervals when many sites show similar patterns.

Our analysis of fire scars (Fig. S2) did not address synchroneity among episodes of burning, which may be caused by climate patterns that promote multiple large fires. Patterns of synchrony do not necessarily correspond with overall fire activity. For example, some studies have shown that fires were larger and regionally more synchronous apparently due to fuel build-up during cold decades, when fire frequency is reduced (8, 9). Other studies, however, have indicated that increased synchrony occurs under increased drought (10). Regardless of the occurrence of regionally synchronous fire years underlying the fire records, the trends in overall rates of burning from both fire-scar and charcoal data show decadal-to-centennial trends that are consistent with climate reconstructions.

Charcoal influx data. Each of the 69 charcoal records was transformed and standardized using a protocol detailed in Power et al. (11) before compositing into a regional charcoal-based index of biomass burning. The transformation, standardization, and summarization methods are designed to highlight the long-term trends in the charcoal data that are characteristic of multiple records. Data were smoothed using local regression using the tricube weight function with 25- and 100-year window (half) widths. Confidence intervals for each composite curve were generated by a bootstrap resampling (with replacement) of individual sites (not samples) over 1,000 replications. Bootstrap confidence intervals for each target point were taken as the 5th and 95th percentiles of the 1,000 fitted values for each target point. This bootstrapping strategy reveals the uncertainty in the smoothed (fitted) values related to the inclusion or not of individual recording sites, and provides a way of gauging the robustness of the fitted curve to the particular distribution of sites in the dataset.

Charcoal decomposition. Charcoal records with data for at least the past 200 y (i.e., with intact core tops) and with at least 17 samples per 1,000 y were selected for further processing to identify individual fire episodes (i.e., one fire event or a series of individual fire events that occurred over several years). Forty-one records met these criteria (Table S1). The selected records were analyzed with CharAnalysis (12). All records were interpolated to their median sample resolution and were not transformed prior to decomposition. Low-frequency (background) charcoal accumulation rates (CHAR) were estimated using a lowess smoother robust to outliers. The background smoothing window-widths were determined by testing alternative window widths and comparing their sensitivity analysis results produced by CharAnalysis. Smoothing window widths that produced a high signal-to-noise index and a high goodness-of-fit index for the noise distribution were selected individually for each record. High-frequency CHAR was calculated using the ratio of interpolated to background CHAR. Threshold values for peak identification were locally defined and based on a percentile cutoff of a noise distribution determined by a Gaussian mixture model. The selection of final peaks were based on those in the 99th percentile of the noise distribution.

Charcoal peak/fire episode frequency. The time series of charcoal peaks were summarized using a kernel-density estimator (13), with bandwidths (25 and 50 y) selected to be comparable with the window widths used for summarizing the other data. We used the same bootstrapping strategy as for the charcoal influx data. Units of the peak-density curve are number of peaks per year per record.

Differences between fire-scar and charcoal data. Fire-scar and charcoal records are complementary across forest types and fire regimes, but also with regard to temporal coverage (4). Fire-scar records generally span centuries and are annually resolved, but the records "fade" before 1500 CE, whereas charcoal records span millennia and integrate information about fire occurrence over years, decades, or centuries, depending on the rate of sedimentation in the record. In addition, charcoal records contain noise relating to taphonomic and site-specific processes that can make identification of biomass burning trends at a single site problematic.

Fire-scar and charcoal records differ in several important respects, however, including their distribution across forest types, registration of fire events, temporal length, and temporal resolution (Fig. 1 *B* and *C*). Fire-scar records are most prevalent in areas with low effective moisture, such as in dry ponderosa pine forests, because the typically low fuel loads promote low intensity burns that frequently scar trees [e.g., (14–16)] but produce low amounts of charcoal that are difficult to detect in the lake-sediment record. In contrast, charcoal records from forests with high effective moisture, such as mixed conifer or subalpine fir forests, are often better resolved because such forests are typically characterized by complex vegetation structures and abundant, continuous fuels that support infrequent, high-severity fires. Ample charcoal is produced during such forest fires, which is incorporated into sediments during and after the fire (17–20).

Lake-sediment records of charcoal are restricted to regions with lakes, and in particular those with continuous deposition of a sufficient rate to ideally provide decadal sampling resolutions. Because local changes that affect vegetation, lake characteristics, erosion patterns, or topography can alter trends in charcoal accumulation, absolute trends in background charcoal at a single lake do not necessarily reflect changes in the local fire regime. By analyzing trends at multiple sites, however, shared characteristics of macroscopic charcoal accumulation rates (CHAR, or charcoal influx) can be used to infer regional-scale changes in fire activity (21, 22). In western forests, where there has been little apparent change in vegetation composition over the last 2,000 y, there is increasing evidence that trends in charcoal influx from nearby sites are correlated with area burned over time (23, 24). When sedimentation rates are high enough (ideally >1 mm/y) and sediment records are sampled continuously, discrete pulses of charcoal can be distinguished from background charcoal variations and used to infer changes in the frequency of fires (12, 25).

Multiple fire-scar and charcoal records thus jointly provide information about widespread variations in fire frequency and biomass burning (10, 26). Although charcoal records are less temporally and spatially precise than fire-scar records, charcoal data can provide a continuous record of burning over millennia. The long-term context provided by such data is especially relevant in light of the magnitude of projected climate changes, which exceed those experienced in recent millennia.

Climate data and treatment. Temperature data were obtained from Mann et al. (27) (Fig. 2*E*). The temperature time series were expressed as anomalies from a 1960–1990 CE long-term mean. The drought reconstruction (Fig. 2*F*) uses updated data from Cook et

al. (28) to calculate a region-wide drought-area index (i.e., the proportion of grid cells with Palmer Drought-Severity Index [PDSI] values less than −1.0). Both series were smoothed using the same approach taken with the charcoal data (i.e., lowess smoothing based on a 100-y window width), and bootstrap confidence intervals were also calculated in a similar fashion, by resampling the individual grid-cell time series, as opposed to individual data values. As is the case for the charcoal data, this approach allows the influence of individual grid points or groups of them on the composite curve to be assessed.

Relationship between biomass burning (charcoal influx) and climate. We used a generalized additive model [Generalized Additive Model (GAM), (29, 30)] to describe the dependence of biomass burning on climate, as represented by the summary curves for charcoal influx, mean annual temperature anomalies [(MAT), (27)] and drought-area index (DAI, 28). We selected this particular modeling framework because it permits the development and display of a smooth function that links a particular response (here, charcoal influx) to a small number of predictor variables (e.g., MAT and DAI). In fitting GAM "surfaces," there is a trade-off between the smoothness of the surface and its fit to individual data points, but this can be controlled by constraining the smoothness of the fitted surface. The summary curves were evaluated at 10-year intervals, and the time span of data used to calibrate the model was 500–1800 CE, thereby avoiding the confounding effects of settlement and fire suppression.

We used the R package mgcv (29) to fit surfaces to the charcoal and climate data using the tensor-product smoother with thin-plate regression splines because the climate data have different units of measurement, and we suspected that the resulting surfaces would be anisotropic (see ref. 29 ch. 5 for a discussion of the practical considerations of GAM fitting). MAT and DAI are also correlated (a situation known as "concurvity" in the GAM literature, $r = 0.62$ for data from 500 to 1800 CE). Although concurvity did not create any noticeable numerical problems here, it did lead to the possibility of identifying multiple models with roughly the same goodness-of-fit, and so we examined a variety of models that included one or the other of the climate variables, as well as interactions between the two. To understand the trade-off between goodness-of-fit and the complexity of the model, we examined the shape of the fitted surface and summary statistics such as the adjusted R^2 and Akaike Information Criterion values for individual models, as well as F-statistics for analysis-of-variance comparisons of a particular model with a "null" model consisting of only the mean value of the charcoal data.

The fitted response surface (Fig. S5) shows a general increase in predicted z-scores of transformed charcoal influx with increasing MAT and DAI, a relationship that is also evident in time series plots of the data (Fig. 2). The model (with equivalent degrees of freedom of 4, 2, and 9 for the MAT, DAI, and interaction terms, respectively) fits the data well ($R^2 = 0.85$; $F = 43.0$; $p < 0.000$), and the residuals to not have any striking features. The surface is relatively smooth, with a slight concavity centered around values of MAT = 0.5 and DAI = 0.35, values that mainly occur between 600 and 800 CE. This feature could be removed by increasing the smoothness of the interaction term, but we elected to keep it in to increase the generality of the fitted surface.

The composite curves used in fitting the GAMs here are quite smooth [i.e., the charcoal, temperature, and drought area series were smoothed using local regression using the tricube weight function with a 100-year window (half) width], which raises the possibility of observing spurious correlation among them, or obtaining inflated estimates of the goodness-of-fit. To examine the impact of pseudoreplication, we refit the model to the composite-curve values sampled at 40-year intervals, the practical upper limit of sample time step for fitting the model (Fig. S6). The model fits the subset data about as well as the 10-year time step data ($R^2 = 0.81$; $F = 10.22$; $p < 0.000$), and captures all of the important features in the predicted charcoal influx series, including the divergence between predicted and observed values after the late 1800s.

A key feature of predictions by the model after the calibration interval end (1800 CE) is the divergence between the decreasing charcoal influx values and the increasing predicted values, beginning in the late 1800s (Fig. 2*C*; Fig. S7 bottom). To visually assess the extent to which these diverging predictions represented "out-of-sample" extrapolations, we examined the scatter plot of MAT and DAI values (Fig. S7, top). This plot suggests that only the 1990 and 2000 CE values of MAT lie substantially outside of the main cloud of points, and that the predicted values for these times represent at most mild extrapolations.

1. Reynolds RV, Pierson AH (1941) *The saw timber resource of the United States,1630-1930. Forest Survey Release 53* (USDA Forest Service, Washington, DC).
2. Ramankutty N, Foley JA (1999) Estimating historical changes in land cover: North American croplands from 1850 to 1992. *Global Ecol Biogeogr* 8:381–396.
3. Hicke JA, Jenkins JC, Ojima DS, Ducey M (2007) Spatial patterns of forest characteristics in the western United States derived from inventories. *Ecol Appl* 17:2387–2402.
4. Swetnam TW, et al. (2009) Multimillennial fire history of the giant forest, Sequoia National Park, U.S.A. *Fire Ecology* 5:120–148.
5. Van Horne ML, Fulé PZ (2006) Comparing methods of reconstructing fire history using fire scars in a southwestern United States ponderosa pine forest. *Canadian Journal for Forest Resources* 36:855–867.
6. Farris CA, Baisan CH, Falk DA, Yool SR, Swetnam TW (2010) Spatial and temporal corroboration of a fire-scar-based fire history in a frequently burned ponderosa pine forest. *Ecol Appl* 20:1598–1614.
7. Loader C (1999) *Local Regression and Likelihood* (Springer, New York).
8. Swetnam TW, Baisan CH (2003) Tree-ring reconstructions of fire and climate history in the Sierra Nevada and southwestern United States. *Fire and climate in temperate ecosystems of the western Americas*, eds Veblen TT, Baker WL, Montenegro G, Swetnam TW (Springer-Verlag, NY), pp 158–195.
9. Trouet V, Taylor AH, Wahl ER, Skinner CN, Stephens SL (2010) Fire-climate interactions in the American West since 1400 CE. *Geophys Res Lett* 37:L04702.
10. Kitzberger T, Brown PM, Heyerdahl EK, Swetnam TW, Veblen TT (2007) Contingent Pacific-Atlantic ocean influence on multicentury wildfire synchrony over western North America. *Proc Nat'l Acad Sci USA* 104:543–548.
11. Power MJ, Marlon JR, Bartlein PJ, Harrison SP (2010) Fire history and the Global Charcoal Database: a new tool for hypothesis testing and data exploration. *Palaeogeogr Palaeocl* 291:52–59.
12. Higuera P, Gavin D, Bartlein P, Hallett D (2010) Peak detection in sediment-charcoal records: impacts of alternative data analysis methods on fire-history interpretations. *Int J Wildland Fire* 19:996–1014.
13. Venables WN, Ripley BD (2002) *Modern applied statistics with S* (Springer Verlag, NY) pp 495.
14. Grissino-Mayer HD, Swetnam TW (2000) Century-scale climate forcing of fire regimes in the American Southwest. *Holocene* 10:213–220.
15. Heyerdahl EK, Brubaker LB, Agee JK (2001) Factors controlling spatial variation in historical fire regimes: a multiscale example from the interior West, USA. *Ecology* 82:660–678.
16. Morgan P, Heyerdahl EK, Gibson CE (2008) Multiseason climate synchronized forest fires throughout the 20th-century, Northern Rockies, USA. *Ecology* 89:717–728.
17. Brunelle A, Whitlock C, Bartlein P, Kipfmueller K (2005) Holocene fire and vegetation along environmental gradients in the Northern Rocky Mountains. *Quaternary Sci Rev* 24:2281–2300.
18. Long CJ, Whitlock C, Bartlein PJ (2007) Holocene vegetation and fire history of the Coast Range, western Oregon, USA. *Holocene* 17:917–926.
19. Gavin DG, et al. (2007) Forest fire and climate change in western North America: insights from sediment charcoal records. *Frontiers in Ecology and the Environment* 5:499–506.
20. Whitlock C, Skinner CN, Bartlein PJ, Minckley T, Mohr JA (2004) Comparison of charcoal and tree-ring records of recent fires in the eastern Klamath Mountains, California, USA. *Canadian Journal of Forest Research* 34:2110–2121.
21. Carcaillet C, et al. (2002) Holocene biomass burning and global dynamics of the carbon cycle. *Chemosphere* 49:845–863.
22. Power MJ, et al. (2008) Changes in fire regimes since the Last Glacial Maximum: an assessment based on a global synthesis and analysis of charcoal data. *Climate Dynamics* 30:887–907.
23. Higuera PE, Peters ME, Brubaker LB, Gavin DG (2007) Understanding the origin and analysis of sediment-charcoal records with a simulation model. *Quaternary Sci Rev* 26:1790–1809.
24. Higuera PE, Whitlock C, Gage JA (2010) Linking tree-ring and sediment-charcoal records to reconstruct fire occurrence and area burned in subalpine forests of Yellowstone National Park, USA. *Holocene* 21:327–341.
25. Gavin DG, Hu FS, Lertzman K, Corbett P (2006) Weak climatic control of stand-scale fire history during the late Holocene. *Ecology* 87:1722–1732.

26. Marlon J, et al. (2009) Wildfire responses to abrupt climate change in North America. *Proc Nat'l Acad Sci USA* 106:2519–2524.
27. Mann ME, et al. (2009) Global signatures and dynamical origins of the Little Ice Age and Medieval Climate Anomaly. *Science* 326:1256–1260.
28. Cook ER, Woodhouse CA, Eakin CM, Meko DM, Stahle DW (2004) Long-term aridity changes in the western United States. *Science* 306:1015–1018.
29. Wood SN (2006) *Generalized Additive Models: An Introduction with R* (Chapman and Hall/CRC Press, FL).
30. Hastie TJ, Tibshirani R (1990) *Generalized Additive Models* (Chapman and Hall, FL).
31. Marlon J, et al. (2008) Climate and human influences on global biomass burning over the past two millennia. *Nature Geosci* 1:697–701.
32. Cleveland WS, Devlin SJ (1988) Locally weighted regression: an approach to regression analysis by local fitting. *Journal of the American Statistical Association* 83:596–610.

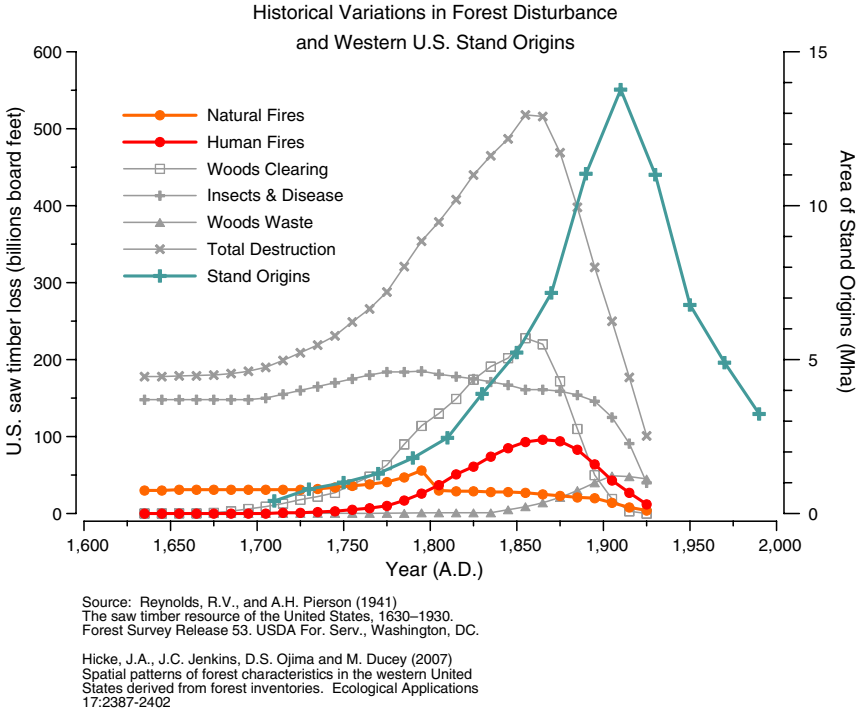


Fig. S1. Historical "drain" on the saw-timber resources of the United States 1630–1930 CE (1). Natural (orange circles) and human-caused fires (red circles) are distinguished from lumber (diamonds), fuelwood (triangles), other disturbances such as insect infestations and wind throw (vertical bars), and from farm clearing (open squares). Stand-origin ages from Hicke et al. (3) are plotted in green, and show the reforestation following the widespread disturbance of the 1800s.

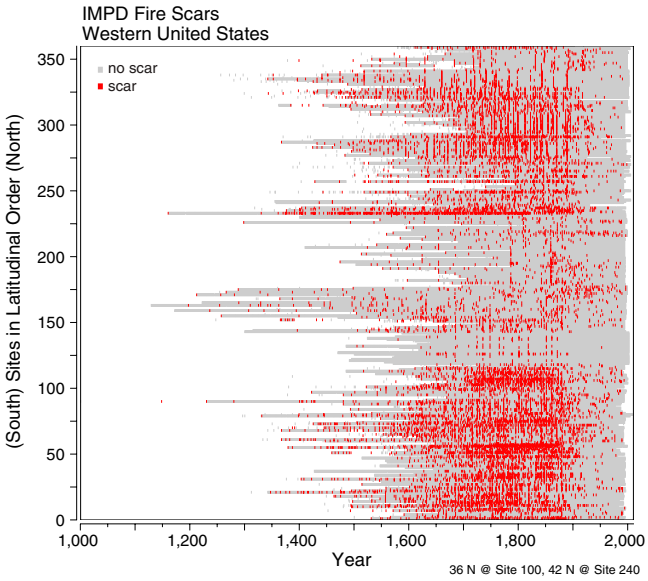


Fig. S2. Fire-scar records from 359 sites spanning the past 1,000 y and arranged in latitudinal order from north (top) to south (bottom). (Site 100 is at 36 N and site 240 is at 42 N) Each site is depicted by a horizontal gray bar; red tick marks represent individual fire scars. Scattered gray tick marks to the left of each bar mark the beginnings of individual tree-ring records. Years when fire was widespread are visible as vertical red streaks in the data. The exclusion and eventual suppression of fire is evidenced after *ca*. 1900 CE by a sharp decline in fire scars. A greater number of fire scars in the bottom half of the graph indicates increased fire frequencies among southern sites. Few fire scars at the middle sites reflect both fewer years of widespread fire compared to the southwest and also the fact that in a mixed fire regime stand-replacing fires destroy some of the evidence of previous fires.

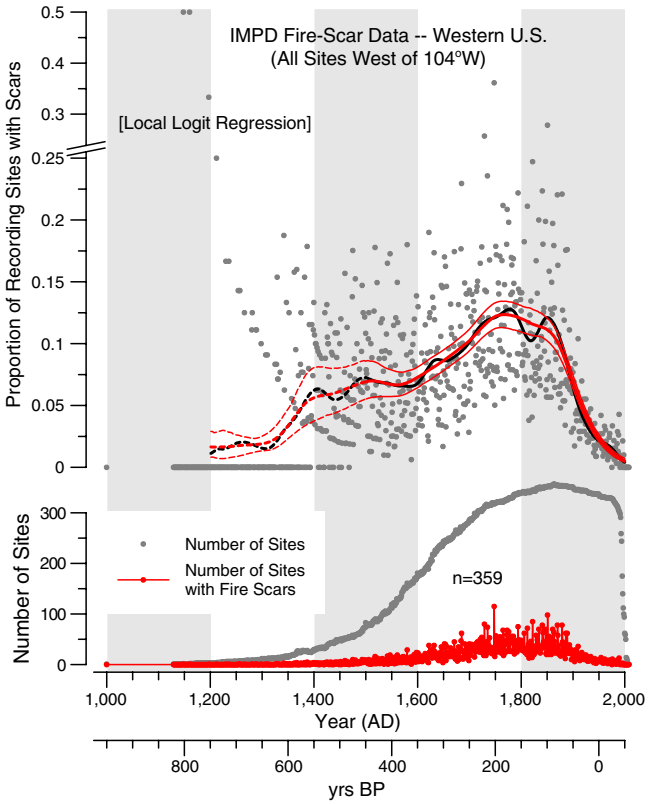


Fig. S3. Fire history from the IMPD fire-scar dataset since 1200 CE showing the proportion of sites recording a fire scar during the past 1,000 y (gray dots, top box), the number of sites each year with recording trees (gray dots, bottom box), and the number of sites each year that have fire scars (red dots). The trend in the proportion of sites recording a fire scar is indicated by a thick red line created by a locally fitted binomial (logit) model. Thin red lines are 95% confidence limits.

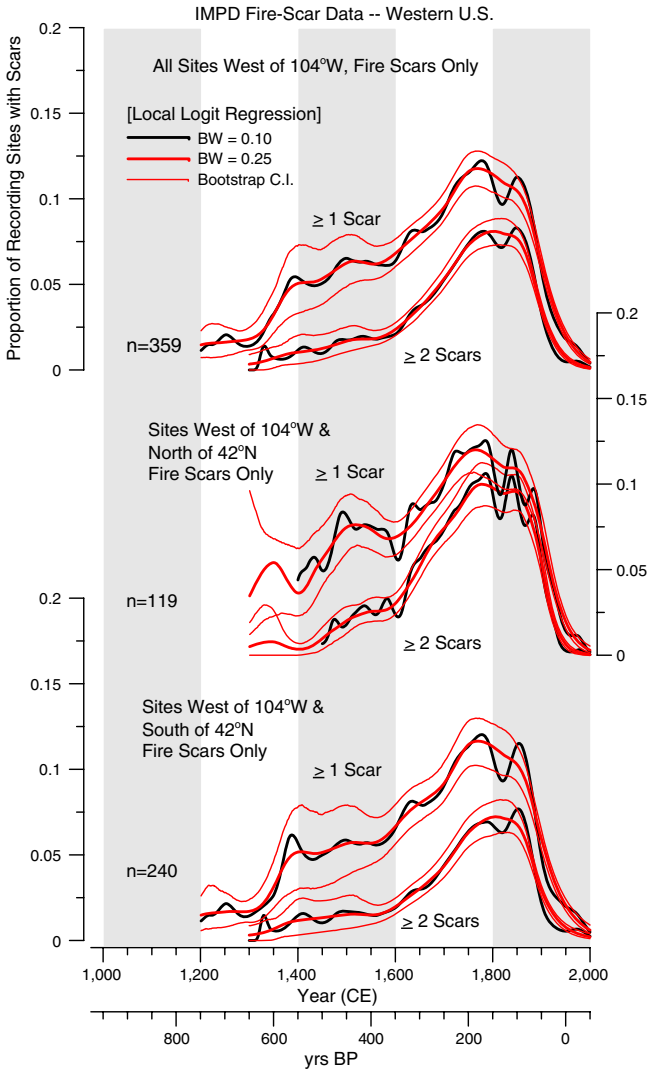


Fig. S4. Comparison of fire history reconstructions from the IMPD fire-scar dataset since 1200 CE using ≥1 (top set of curves in each box) and ≥2 (bottom set of curves in each box) scars to fit a local regression model using a bandwidth of 10 (black line) and 25 (thick red line) years for (*i*) the western United States as a whole; (*ii*) only sites north of 42 °N; and (*iii*) only sites south of 42 °N. Thin red lines are 95% confidence limits.

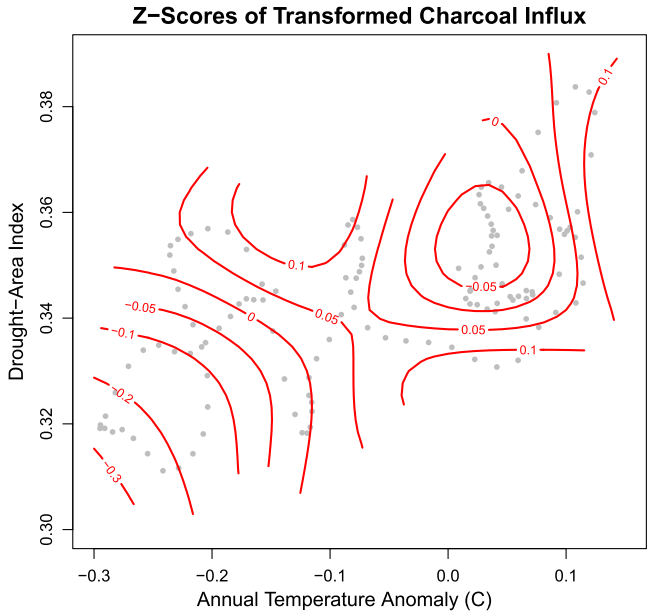


Fig. S5. GAM-fitted response surface showing the relationship between the summary curve of standardized and transformed charcoal influx values and the summary curves of MAT and DAI. Gray dots show the individual data points for the calibration interval (500–1800 CE).

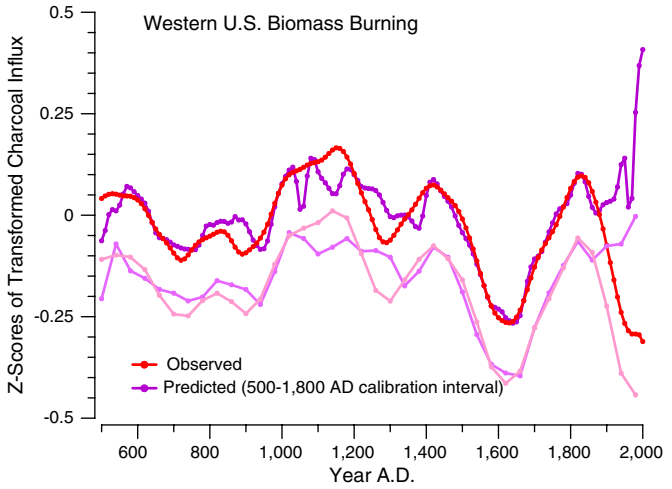


Fig. S6. Observed (red) and predicted (dark purple) values of the standardized and transformed charcoal influx. The corresponding values for a subsampled (40-y) dataset are plotted in pink (observed) and light purple (predicted), respectively, offset by −0.10 Z-score units for clarity.

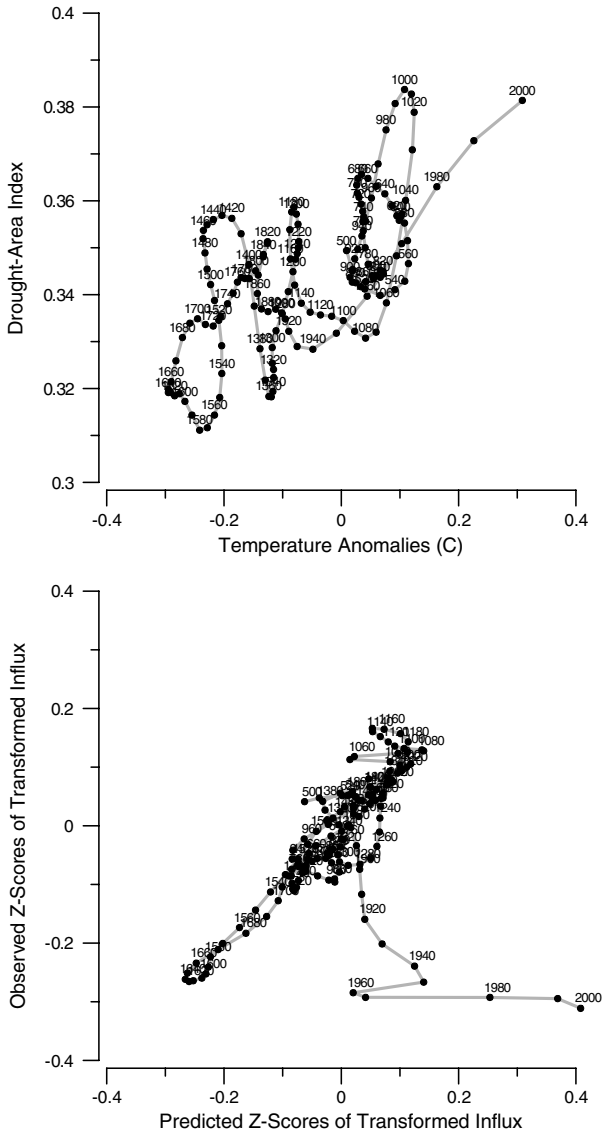


Fig. S7. Scatter plot of MAT and DAI, labeled by observation year (top). The plot shows that only the values for 1990 and 2000 (and perhaps 1890) CE lie outside of the main clound of points, and would generate mild extrapolations. Scatter plot of observed and predicted standardized and transformed charcoal influx (bottom), showing the divergence of observed and predicted (by climate) values in the 20th century.

Table S1. Site names and locations from GCD v1 and additional records from coauthors that are included in the charcoal analyses

Site ID	Site name	Peaks	Latitude	Longitude	Elevation (m)
1	Abalone Rocks Marsh	no	33.9564	−119.9767	1
2	Alamo Bog	yes	35.9111	−106.5838	2,630
3	Baker Lake	yes	45.8919	−114.2619	2,300
4	Barrett Lake	yes	37.5957	−119.0066	2,816
5	Battle Ground Lake	yes	45.8000	−122.4917	154
6	Beaver Lake	yes	44.9175	−123.3050	69
7	Beef Pasture	no	37.4167	−108.1500	3,060
8	Bluff Lake	yes	41.3467	−122.5575	1,921
9	Bolan Lake	yes	42.0200	−123.4600	1,637
10	Burnt Knob	yes	45.7044	−114.9867	2,250
11	Cambell Lake	yes	41.5333	−123.1050	1,750
12	Cedar Lake	no	41.2075	−122.4954	1,740
13	Chihuahueños Bog	yes	36.0472	−106.5083	2,925
14	Coast Trail Pond	yes	37.9853	−122.8000	230
15	Como Lake	no	37.5500	−105.5000	3,523

Site ID	Site name	Peaks	Latitude	Longitude	Elevation (m)
16	Crane Lake	no	36.7167	−112.2167	2,590
17	Crater Lake	yes	41.3836	−122.5778	2,288
18	Crevice Lake	yes	45.0000	−110.5780	1,713
19	Cygnet Lake	yes	44.6628	−110.6161	2,530
20	Dead Horse Lake	yes	42.5606	−120.7781	2,248
21	DeHerrera Lake	yes	37.7417	−107.7083	3,343
22	East Lake	yes	37.1779	−119.0277	2,863
23	East Sooke Fen	no	48.3519	−123.6817	155
24	Five Lakes	no	48.0819	−118.9294	780
25	Forest Pond 1	no	43.4717	−109.9389	2,797
26	Forest Pond 2	no	43.4389	−109.9500	2,766
27	Foy Lake	yes	48.1658	−114.3592	1,006
28	Frying Pan	no	38.6167	−111.6667	2,720
29	Glenmire Lake	yes	37.9933	−122.7770	399
30	Head Lake	no	37.7000	−105.5000	2,300
31	Hidden Lake	yes	40.5100	−106.6100	2,710
32	Hoodoo Lake	yes	46.3206	−114.6503	1,770
33	Hunter's Lake	no	37.6083	−106.8444	3,516
34	Jicarita Bog	yes	36.0708	−105.5889	3,207
35	Lake Oswego	yes	45.4111	−122.6661	30
36	Lily Lake	yes	41.9758	−120.2097	2,042
37	Little Lake	yes	44.1680	−123.5835	703
38	Little Molas Lake	yes	37.7417	−107.7083	3,370
39	Lost Lake	yes	45.8242	−123.5792	449
40	Lower Gaylor Lake	yes	37.9086	−119.2863	3,062
41	Martins Lake	no	47.7138	−123.5400	1,415
42	Montezuma Well	no	34.0000	−112.0000	1,125
43	Moose Lake	no	47.8830	−123.3500	1,508
44	Mumbo Lake	yes	41.1913	−122.5092	1,860
45	Park Pond 1	no	43.4681	−109.9594	2,705
46	Park Pond 2	no	43.4500	−109.9408	2,714
47	Park Pond 3	no	43.4592	−109.9200	2,739
48	Patterson Lake	yes	41.3867	−120.2236	2,743
49	Pintlar Lake	yes	45.8406	−113.4403	1,921
50	Pixie Lake	no	48.5964	−124.1967	70
51	Porter Lake	no	44.4478	−123.2428	73
52	Posy Lake	no	37.9500	−111.7000	2,653
53	Reservoir Lake	no	45.1300	−113.4600	2,161
54	San Joaquin Marsh	no	33.6583	−117.8583	2
55	Sanger Lake	yes	41.9021	−123.6465	1,547
56	Siesta Lake	no	37.8500	−119.6667	2,430
57	Slough Creek Pond	yes	44.9183	−110.3467	1,884
58	Swamp Lake	no	37.9500	−119.8167	1,554
59	Taylor Lake CA	yes	41.3614	−122.9675	1,979
60	Taylor Lake OR	yes	46.1006	−123.9067	6
61	Three Creeks	yes	44.0990	−121.6273	1,996
62	Todd Lake	yes	44.0277	−121.6846	1,875
63	Trail Lake	yes	44.2800	−110.1700	2,362
64	Tumalo Lake	yes	44.0218	−121.5438	1,536
65	Upper Rocket Creek Bog	no	47.0405	−115.8888	1,710
66	Upper Squaw lake	yes	42.0333	−123.0150	930
67	Warner Lake	no	44.2461	−122.9575	590
68	Whyac Lake	no	48.6722	−124.8444	15
69	Wildcat Lake	yes	37.9684	−122.7851	67